

Effects of structure of anodic TiO₂ nanotube arrays on photocatalytic activity for the degradation of 2,3-dichlorophenol in aqueous solution

Hai-chao Liang, Xiang-zhong Li*

Department of Civil and Structural Engineering, The Hong Kong Polytechnic University,

Hunghom, Kowloon, Hong Kong, China

**Corresponding author. Tel.: +852 2766 6016; fax: +852 2334 6389.*

E-mail address: cexzli@polyu.edu.hk (X.Z. Li).

Abstract

In this study titanium dioxide nanotube (TNT) arrays were prepared by an anodic oxidation process with post-calcination. The morphology and structure of the TNT films were studied by FESEM, XRD, and XPS. Photocatalytic activity of the TNT films was evaluated in terms of the degradation of 2,3-dichlorophenol in aqueous solution under UV light irradiation. The effects of the nanotube structure including tube length and tube wall thickness, and crystallinity on the photocatalytic activity were investigated in details. The results showed that the large specific surface area, high pore volume, thin tube wall, and optimal tube length would be important factors to achieve the good performance of TNT films. Moreover, the TNT films calcined at 500 °C for 1 h with the higher degree of crystallinity exhibited the higher photocatalytic activity than other TNT films calcined at 300 °C and 800 °C. Consequently, these results indicate that the optimization of TiO₂ nanotube structures is critical to achieve the high performance of photocatalytic reaction.

Keywords: Anodic oxidation; Photocatalysis; TiO₂ nanotube arrays; 2,3-Dichlorophenol.

1. Introduction

Photoactive semiconductor, titanium dioxide (TiO_2), has attracted great attention owing to their potential applications in the areas of electronics, optics, catalysis, biotemplating, and gas-sensing materials [1-4]. Many researches have proven that multidimensional TiO_2 has the higher photochemical reactivity than that of bulk TiO_2 particles [5-7]. Advances in the nanoscale technology facilitated the synthesis of highly-ordered and multidimensional structured materials. In recent years, considerable efforts have been focused on new techniques for synthesizing titania with a unique nanoarchitecture consisting of vertically-oriented, immobilized, highly-ordered and high-aspect ratio nanotubes such as hydrothermal treatment [8,9], template synthesis [10], and anodic oxidation [11]. Kasuga et al. [8] used a hydrothermal process for treatment of titania particles in NaOH solution at 110 °C and then washed with water and hydrochloric acid to form titania nanotubes. They reported that this washing procedure was critical in the formation of titania nanotubes. However, Du et al. [9] claimed that the resulting nanotubes were not TiO_2 but rather $\text{H}_2\text{Ti}_3\text{O}_7$. Among the various synthetic methods, the template method has been demonstrated to be effective to produce TiO_2 with a hollow structure. In which the TiO_2 nanoparticles were either deposited within the preformed tubular templates such as porous polymer latex and anodic aluminum oxide [10,12] by the sol-gel, electrochemical deposition or electrospinning methods to form one-dimensional TiO_2 hollow structures. However, these methods either are complicated due to the use of templates or involve some rigorous chemical processes. Alternatively, the anodization process could be a more simple technique to synthesize the highly-ordered TiO_2 nanotubes. Zwilling et al. in 1999 [11] first reported the anodization of titanium for an important surface treatment in chromic acid solution with and without hydrofluoric acid addition. Grimes and his group in 2001 synthesized the uniform and highly-ordered TiO_2 nanotube arrays by anodic oxidation of a pure titanium sheet in an aqueous

electrolyte containing 0.5 to 3.5 wt% hydrofluoric acid [13] and reported the influence of electrolyte composition, pH, and reaction temperature on the formation of TiO₂ nanotubes [14]. They have successfully employed these well aligned TiO₂ nanotubes in the application of hydrogen sensor and water photocleavage [15,16].

TiO₂ nanotubes as photocatalysts also begin to be paid significant attention in environmental applications [17,18], yet to date there are only limited reports about the effect of their structures on the photocatalytic behaviors. Although Lai et al. [19] investigated the effect of crystallinity and length of TiO₂ nanotubes on the photodegradation of methylene blue in aqueous solution, but they ignored the effect of tube wall thickness on the photocatalytic ability, which might play a key role on the charge transfer and the separation of electro-hole pairs. Calcination temperature is another key parameter to determine the overall photocatalytic activity of TiO₂ catalysts. Although many reports published within last years involved the effects of calcination temperature on the photocatalytic activity of TiO₂ nanotubes, the results did not agree between each other. For example, Zhu et al. in 2004 [20] found that the as-prepared titanate nanotubes without calcination exhibited decent photocatalytic activity for the photocatalytic oxidation of sulforhodamine, but Yu et al. in 2006 [21] claimed that no any photoactivity of TiO₂ nanotubes obtained by hydrothermal technique was observed when the calcination temperature is below 300 °C. Therefore, it is necessary to further investigate the influence of calcination temperature on the photoactivity of the anodic TiO₂ nanotubes.

The aim of this study is at detailing the photoactivity of TiO₂ nanotube films as a main function of structure factors including pore size, tube length, tube wall thickness, and crystallinity, in which 2,3-dicholophenol (2,3-DCP) was used as a model chemical and its degradation with different TiO₂ nanotube films under UV illumination was investigated in aqueous solution. From the results of this study it can be better understand the photocatalytic activity of TNT films with structural specificity and functional novelty.

2. Experimental

2.1. Materials

Titanium foils (140 μm thickness, 99.6% purity) were purchased from Goodfellow Cambridge Ltd. Ammonium fluoride (NH_4F), H_2SO_4 , and 2,3-DCP were purchased from Aldrich Chemical Company. Other chemicals were obtained as analytical grade reagents and used without further purification. Deionized distilled water (DDW) was used throughout the experiments.

2.2. Anodic oxidation process

A large piece of raw titanium (Ti) foil was cut into small rectangle pieces of 30 mm \times 10 mm, which were ultrasonically cleaned in an acetone-ethanol solution and then washed with DDW prior to anodization. An anodic oxidation process was conducted in a dual-electrode reaction chamber, in which the cleaned Ti foil was used as the anode and a platinum (Pt) foil of the same size was applied as the cathode. Two electrodes with a distance of 2 cm were submerged into an electrolyte solution containing 0.1M NH_4F at pH 1.5 adjusted by H_2SO_4 and a DC electrophoresis power supply (EPS 600) was used to provide different electrical potentials between two electrodes during the anodic oxidation reaction. The resulting TiO_2 nanotubular array-films on Ti substrate were then rinsed by DDW and subsequently calcined in air at different temperatures of 300, 500 and 800 $^\circ\text{C}$ for 1 h, respectively.

2.3. Characterization of TiO_2 nanotube arrays

The surface morphology of the prepared samples was first examined using the field-emission scanning electron microscopy (FESEM; JSM6300, Japan). To determine the phase composition and crystal structure of the catalysts, X-ray diffraction (XRD) measurement was carried out at room temperature using a Bruker D8 Discover XRD with diffracted beam graphite

monochromator at 50 kV and 40 mA (Cu K α with $\lambda = 1.54187 \text{ \AA}$). Information on the chemical states of the samples was obtained from X-ray photoelectron spectroscopy (XPS, SKL-12), in which all the binding energy referencing to the C1s peak at 284.6 eV of the surface adventitious patterns were recorded.

2.4. Photocatalytic reaction experiments

A photoreaction system consists of a glass reactor with a magnetic stirrer and an 8-W medium pressure mercury lamp (Institute of Electrical Light Source, Beijing, China) with the main emission at 365 nm as an external UV light source. A distance between the lamp and the top surface of the solution is 6 cm.

The photocatalytic activity of the TNT films was evaluated via the photodegradation of 2,3-DCP in aqueous solution, while a TiO₂ thin film on Ti substrate was also prepared by a sol-gel method according to the literature [22] and used for comparison. A set of photocatalytic degradation experiments was performed with the following procedure: a TNT or TiO₂ film with an area of 3 cm² was placed in 25 mL of aqueous 2,3-DCP solution with an initial concentration of 20 mg L⁻¹; prior to the photoreaction, the reaction solution was magnetically stirred in the dark for 60 min to reach adsorption/desorption equilibrium; then the reaction with stirring was irradiated by the UV light from the top vertically; during the photoreaction, samples were collected at different time intervals for analysis.

2.5. Analytical methods

The concentration of 2,3-DCP in aqueous solution was determined by HPLC (Finnigan P4000 Model), in which a reversed phase column (RESTEK Pinnacle II, C18) with a particle size of 5 μm , the length of 250 mm, and an inner diameter of 4.6 mm was used and a mobile phase of acetonitrile:water:acetic acid (69:30:1, v:v) flowed at 0.8 mL min⁻¹. The 2,3-DCP concentration

was determined by a UV detector (UV 6000LP) at 200 nm.

3. Results and discussion

3.1. Morphology of TNT films

The formation of TiO₂ nanotube arrays on the surface of titanium depends on both reactions of electrochemical etching and chemical dissolution. Since the interaction between two reactions could significantly affect the morphology and structure of TNT films, it would be a key factor to influence the photocatalytic activity of catalysts. In this study aqueous 0.1M NH₄F solution was used as an electrolyte to prepare seven TNT film samples (S1-S7) under various anodization conditions as summarized in Table 1. A TiO₂ thin film on Ti substrate was also prepared by the sol-gel method for comparison. These as-prepared samples were then calcined at 500 °C for 1 h. The calcined final samples were first examined by FESEM and their images are shown in Fig. 1. It can be seen that the TiO₂(500) film had a nonporous structure and its thickness is about 1 μm. The SEM images of TNT films showed that the TNT-S1(500) anodized at a low voltage of 10 V for 1 h had only a few pits; the TNT-S2(500) at 15 V showed a partial porous structure; and the TNT-S3(500) at 18 V and TNT-S5(500) at 25 V had complete porous structures with well-aligned nanotube arrays. These results indicated that the formation of the well-aligned TNT arrays at the voltage of below 18 V was difficult due to weak electrochemical etching reaction and 25 V would be a sufficient electrical potential to well develop the TNT arrays on the Ti surface.

[Table 1]

[Fig. 1]

To study the effect of anodizing time on the structure of the nanotubes, three experiments were conducted at 25 V for different times of 0.3, 1 and 10 h. It is found that the length of TiO₂ nanotubes was significantly increased with the increased anodizing time (0.20 μm for 0.3 h, 0.31 μm for 1 h and 2.38 μm for 10 h), respectively. These results indicated that the tube length was significantly affected by anodizing time with a good agreement with the literature [14].

Mor et al. [15] have reported that the thickness of the anodic nanotube walls can be controlled via anodization bath temperature. To obtain the TiO₂ nanotubes with different wall thickness to compare their photocatalytic activity, the TNT-S7(500) was anodized at a lower temperature of 5 °C while other TNT films were anodized at 23 °C. It was found that TNT-S7(500) had a highly-disturbed porous structure with similar nanotube length, but a thicker wall of ~50 nm compared to TNT-S5(500) (28 nm). The increased thickness of nanotube walls should be a consequence of using the lower anodization temperature. Although the formation of TiO₂ nanotubes is a result of the competition between the electrochemical etching of Ti and the chemical dissolution of TiO₂ occurring in the electrolyte solution during anodization [16], the chemical dissolution would be a limiting factor for the growth of nanotube length and wall, depending on the solution temperature. It is therefore believed that at low temperature the rate of the oxide dissolution reaction was more slowly than that of Ti etching, thus resulting in the formation of thicker nanotube walls.

3.2. Characteristics of TNT films

One XRD pattern of Ti foil and four XRD patterns of TNT-S5 annealed at different temperatures from 300 to 800 °C are shown in Fig. 2. It can be seen that the nanotubes without calcination (pattern 2) maintained an amorphous structure, which means that the low-voltage anodization only formed amorphous TiO₂ nanotubes, but not lead to TiO₂ crystallization. The patterns 3-5 show the crystallization calcined at 300, 500 and 800 °C, respectively, in which amorphous regions was gradually crystallized to form anatase/rutile phases. Further observation

shows that the relative intensities of anatase and rutile diffraction peaks in each product are different for the new TiO₂ layer obtained at different calcination temperature. It can be seen that at 300 °C (pattern 3), only a small diffraction peak of anatase at 25.35° (101) but no any the rutile diffraction peaks occurred. This result reflects that the phase transformation to anatase or rutile was not fully achieved at 300 °C and still contained some inactive amorphous phase. While calcined at 500 °C, the sample (pattern 4) possessed characteristic peaks at 25.35° (101), 27.5° (110), 36.1° (101), 48.1° (200), 54.3° (211), and 69.8° (220), respectively. According to the XRD indexation, the crystal form of TNT is a mixture of rutile and anatase phases in good agreement with previous reports [23,24]. According to the equation $f_r = 1.26I_r / (I_a + 1.26I_r)$ [25], the mass fraction of rutile (f_r) in this sample was calculated by measuring the intensity of the strongest (110) and (101) diffraction peaks of rutile (I_r) and anatase (I_a), respectively to be ca. 52%. At 800 °C (pattern 5), the diffraction peak of anatase (101) disappeared completely and the rutile peak (110) became very strong. It is reasonable to infer from these results that the anatase phase was transformed into rutile phase during heat-treatment at high temperature. Furthermore, the critical nanotube disintegration after calcination at 800 °C can be observed in the SEM image of Fig. 3. It is worth mentioning that Varghese et al. [26] observed a similar morphology as that the nanotube structure completely collapsed at 880 °C leaving dense rutile crystallites.

[Fig. 2]

[Fig. 3]

To study the surface composition and chemical states of the obtained nanotubes, the TNT-S5(500) was also analyzed by XPS and its XPS spectra are shown in Fig. 4. The individual peaks of O 1s at 529.5 eV and Ti 2p at 458.2 and 463.9 eV can be clearly seen in the high resolution spectra, which mean that chemical state of the sample is Ti⁴⁺ bonded with oxygen (Ti⁴⁺-O). In

the meantime, the spectra show a trace amount of carbon (C 1s), which should be ascribed to the adventitious hydrocarbon from the XPS sample preparation. In our experiment no evidence of other trace elements from electrolyte solution such as nitrogen (N), fluorine (F), or sulfur (S) was obtained, which confirmed that the elements of N, F, and S were not incorporated into the TiO₂ crystal lattice during the anodization, although these elements were constrained in the electrolyte solution as NH₄F and H₂SO₄. Furthermore, the XRD spectra of TNT samples also give no indication of any TiO_xF_y, TiO_xN_y or TiO_xS_y existing in the samples, which can confirm that the electrolyte elements did not enter either rutile or anatase lattice in such a low-voltage anodization process.

[Fig. 4]

3.3 Effect of surface structures of TNT films

The photocatalytic activity of the anodized TNT films with different surface structures (TNT-S1(500), TNT-S2(500), and TNT-S5(500)) was evaluated in the photodegradation of 2,3-DCP in aqueous solution under UV light irradiation and the TiO₂ film with a same area of 3 cm² was also prepared and heated at the same temperature of at 500 °C for comparison, as shown in Fig. 5. The semi-log graphs of the 2,3-DCP degradation with different TNT films versus irradiation time yield straight lines, indicating the pseudo-first-order reaction kinetics. The reaction rate constants (k) were evaluated from the experimental data using a linear regression. In all cases R^2 (correlation coefficient) values are higher than 0.96, which indicate that the exponential model can well describe the kinetics for degradation of 2,3-DCP in this process.

It can be clearly observed from Fig. 5 that the TiO₂(500) film showed the lowest photocatalytic activity with a corresponding k value of $1.5 \times 10^{-3} \text{ min}^{-1}$. However, The TNT films (TNT-S1(500), TNT-S2(500), and TNT-S5(500)) demonstrated the higher photocatalytic activity as compared to

TiO₂(500) film. Among them, TNT-S5(500) showed the highest photoactivity with corresponding k value of $8.0 \times 10^{-3} \text{ min}^{-1}$, while TNT-S2(500) had $k = 4.1 \times 10^{-3} \text{ min}^{-1}$ and TNT-S1(500) had $k = 3.3 \times 10^{-3} \text{ min}^{-1}$. This enhancement of photoactivity can be attributed to the difference of surface structures between the ordinary TiO₂ film and anodic TNT films. The TiO₂(500) thin film had a nonporous and tight solid structure with low specific surface area and poor charge mobility (see Fig. 1), thus resulting in the low activity. In contrast, larger specific surface area of anodic TNT films allow more aqueous reactants to be adsorbed onto the outer and also inner surfaces of the photocatalysts, while the higher pore volume results in a faster diffusion of various aqueous species during the photocatalytic reaction. All these factors contributed to the enhancement of photocatalytic activity. However, it should be noted that the factors resulting in the high photoactivity were strongly dependent upon the pore size and nanotubular structure of TNT films. As shown in Fig. 1, TNT-S1(500) had only a few pits and was not a porous structure; TNT-S2(500) showed a partial porous structure; and TNT-S5(500) had a complete porous structure with well-aligned nanotube arrays. These hollow and well-aligned nanotube arrays can produce a higher special surface area and favor the charge mobility, thus achieving the higher photoactivity. If it is believed that the degree of perfect tube-like structure benefits to form the large surface area and high pore volume, the well-aligned nanotubular structure of TNT-S5(500) is positively favorable to the highest photocatalytic activity as compared to other anodic samples.

[Fig. 5]

3.4 Effect of the length of TiO₂ nanotubes

To evaluate the effect of TiO₂ nanotube length on its photocatalytic activity, the degradation of aqueous 2,3-DCP solution in the presence of TNT samples (TNT-S3(500), TNT-S5(500), and TNT-S6(500)) was carried out under UV light irradiation. These TNT films had similar nanotube

wall thickness, but different nanotube lengths ($\sim 0.31 \mu\text{m}$ for TNT-S3(500) and TNT-S5(500), and $\sim 2.38 \mu\text{m}$ for TNT-S6(500)). Also, the calcined TiO_2 film was used for comparison and the experimental results are shown in Fig. 6. As the mentioned above, the TiO_2 (500) film showed the lowest photocatalytic activity due to its nonporous solid structures and low specific surface area, while TNT-S3(500), TNT-S5(500), and TNT-S6(500) demonstrated the higher photocatalytic activity, which can be attributed to the combination of several factors including the large surface area, hollow interior wall, and porous structures. Considering the similar nanotubular structure and approximate wall thickness of three samples (TNT-S3(500), TNT-S5(500), and TNT-S6(500)), the surface area of these TNT films depends on the tube length and should play an important role in enhancing the photocatalytic activity of TNT films.

It can be noted that TNT-S3(500) and TNT-S5(500) with the similar nanotube length of $\sim 0.31 \mu\text{m}$ exhibited a similar degree of 2,3-DCP degradation (90% and 93%, respectively), which were higher than that (81.2%) of TNT-S6(500) with the longer nanotubes of $2.38 \mu\text{m}$. The fact that the photoactivity declined with the longer nanotubes may be attributed to the limited depth of incident photon penetration through the nanotubes and the diffusion of reactant inside nanotubes [27]. It is generally believed that both the absorption of the incident photons and adsorption of 2,3-DCP by the TNT films should increase with the increasing of tube length, which are beneficial to achieve a greater photocatalytic degradation rate. However, the light intensity usually attenuates as it penetrates into the solid photocatalyst film. If the length of nanotubes is longer than the effective depth of light penetration, the lower part of nanotubes has a difficulty to well absorb UV light. It means that amount of absorbed incident photons by the TNT films will not further increase when the tube length exceeds a certain range. Actually, the existence of the optimal thickness of TiO_2 films for degrading organic pollutants in water [28] also demonstrated the limitation of the UV light penetration. In this study, the length of nanotubes corresponds to the thickness of films mentioned in previous literature [27,29]. On the other hand, the diffusion of

species controlling reactions takes place not only on the outer surface of TiO₂ nanotubes but also on the inner walls due to the capillarity structure. Under a stirring condition, the external diffusion may be improved, but the internal diffusion within the nanotubes is hardly affected. Therefore, the longer nanotubes have a slower internal diffusion for reactants, which is detrimental to the reaction rate.

[Fig. 6]

3.5 Effect of the wall thickness of TiO₂ nanotubes

As we know, the large surface area of the nanoporous film can enhance the adsorption of pollutants in aqueous solution and also enables light harvesting with a higher amount of photogenerated charge. Electron transport from the interband states or excitants to the surface is a limiting factor in the performance of these porous nanocrystallines, and the trapping of electrons to the surface is extremely dependent on the crystal size [30]. Therefore, it is very valuable to investigate the effect of wall thickness of TiO₂ nanotubes on the photocatalytic activity. However, the reported data related to the effect of nanotube wall thickness on the photocatalytic activity are quite limited.

Fig. 7 compared the efficiency of 2,3-DCP degradation with three TNT films (TNT-S3(500), TNT-S5(500) and TNT-S7(500)), which had the similar nanotube length of ~0.31 μm but different nanotube wall thickness (~30 nm for TNT-S3(500), ~28 nm for TNT-S5(500), and ~50 nm for TNT-S7(500)). In this set of experiments, due to the well-aligned tube-like structures, TNT-S3(500), TNT-S5(500), and TNT-S7(500) showed the higher activity as compared with TiO₂(500) thin film. Among them TNT-S5(500) achieved the highest 2,3-DCP removal of up to 93% after 300 min UV illumination, which is about 2.6 times of that by the TiO₂(500) thin film. However, TNT-S7(500) achieved the degradation of 2,3-DCP by 78.5% only during the same

period. The results showed that the TNT films with the thinner nanotube wall achieved the higher removal of 2,3-DCP after 300 min UV illumination in an order of TNT-S5(500) > TNT-S3(500) > TNT-S7(500). It may be understood that when TiO₂ semiconductor is irradiated, electrons and holes are generated, but always recombine immediately. If the electrons and holes created do not recombine rapidly, they need to be either trapped in some metastable states or migrate to the semiconductor surface separately. As the thickness become smaller, the surface states increase rapidly, thus, reducing the nonradiative surface recombination [31]. In other words, the thinner wall is easier for the excited electrons migrate from bulk to surface and provides more accessible carriers trapped on catalyst surface for the photocatalysis thus, enhancing the photocatalytic efficiency. Comparing the affecting factors of nanotube wall thickness and length, it seems that the wall thickness is a more important parameter influencing the overall photocatalytic efficiency of the 2,3-DCP decomposition reaction than the tube length.

[Fig. 7]

3.6 Effect of the calcination temperature

The photocatalytic activity of the TiO₂ nanotubes after calcination at different temperatures was evaluated in terms of 2,3-DCP photodegradation in aqueous solutions. Fig. 8 shows that the 2,3-DCP decay rate is strongly dependent on the calcination temperatures. It can be seen that the TNT film without calcination had very poor photocatalytic activity due to the amorphous structure. When calcined at 300 °C, however, the TNT film showed a certain degree of photocatalytic activity with a kinetic rate constant (k) of ca. 2.5×10^{-3} , which resulted from a low degree of crystallization of anatase phase [32]. This result is different from the report by Yu et al. [21], in which they found that the titanate nanotubes formed by hydrothermal method, below the calcination temperature of 300 °C, showed no photocatalytic activity for the photooxidation of

acetone in air. This difference in photocatalytic activity may be attributed to the different experimental conditions and the different crystal structure prepared by different methods. In present study, The TNT film calcined at 500 °C achieved the highest degree of 2,3-DCP degradation with an apparent kinetic rate constant (k) of ca. 8.9×10^{-3} . This superior activity of the sample may be ascribed not only to their large specific surface area and high pore volume, but also the optimum crystallinity of anatase/rutile phase developed at this temperature. With further increasing the calcination temperature to 800 °C, the photocatalytic activity of the TNT decreased significantly with a much lower k value of ca. 1.9×10^{-3} only. The decline of the photocatalytic activity for the TNT film calcined at the higher temperatures could be explained by the loss of anatase phase (see the XRD pattern in Fig. 2) together with severe nanotube disintegration (see the SEM images in Fig. 3). It is worth noting that when Qamar et al. [33] investigated the influence of calcination temperature (from 300 to 900 °C) on the photocatalytic activity of titanate nanotubes, they also found that the as-prepared nanotubes calcined at 400-500 °C showed the best activity for the degradation of the dye followed by a decrease at higher temperatures, which is in good agreement with our result.

[Fig. 8]

4. Conclusions

In this study different TiO₂ nanotube arrays were prepared by the constant-potential anodization successfully. XRD and XPS spectra of TNT-S5(500) confirmed that the anodic nanotubes contained TiO₂ only without incorporation of any electrolyte elements such as N, F, and S. All the anodic TNT films exhibited the better photocatalytic activity for 2,3-DCP degradation in aqueous solution than that of the traditional TiO₂ film prepared by the sol-gel method and an optimal annealing temperature was found to be at 500 °C. Based on the

experimental results, it can be concluded that morphology and structure of TiO₂ nanotubes including tube wall thickness and tube length are important factors to influence the efficiency of the photocatalysis. Photocatalytic activity of TiO₂ nanotubes decreased with the increased nanotube wall thickness but was not proportional to their length. Comparing these factors, it was found that the nanotube wall thickness is a more important parameter to influence the overall efficiency of the 2,3-DCP degradation reaction. On the other hand, the crystalline phase is also one of key factors affecting the photocatalytic activity of TiO₂ nanotubes. The TNT-S5(500) sample calcined at 500 °C for 1 h with a high degree of crystallinity exhibited the highest photocatalytic activity as compared with other samples calcined at 300 °C and 800 °C. Based on this study, it may be inferred that the surface structure, nanotube length, nanotube wall thickness and calcination temperature of an anodic TiO₂ nanotube film play very crucial roles in determining its photocatalytic activity.

Acknowledgements

The authors wish to acknowledge the support of the Research Committee of The Hong Kong Polytechnic University by providing a PhD scholarship for H. C. Liang.

References

- [1] Z. Tun, J.J. Noel, D.W. Shoesmith, Electrochemical modification of the passive oxide layer on a Ti film observed by in situ neutron reflectometry, *J. Electrochem. Soc.* 146 (1999) 988-994.
- [2] H. Yamashita, Y. Ichihashi, S.G. Zhang, Y. Matsumura, Y. Souma, T. Tatsumi, M. Anpo, Photocatalytic decomposition of NO at 275 K on titanium oxide catalysts anchored within zeolite cavities and framework, *Appl. Surf. Sci.* 121-122 (1997) 305-309.

- [3] R. Rodriguez, K. Kim, J.L. Ong, *In vitro* osteoblast response to anodized titanium and anodized titanium followed by hydrothermal treatment, *J. Biomed. Mater. Res. A* 65 (2003) 352-358.
- [4] A.M. Azad, S.A. Akbar, S.G. Mhaisalkar, L.D. Birkefeld, K.S. Goto, Solid-state gas sensors: A review, *J. Electrochem. Soc.* 139 (1992) 3690-3704.
- [5] J.M. Macak, M. Zlamal, J. Krysa, P. Schmuki, Self-organized TiO₂ nanotube layers as highly efficient photocatalysts, *Small* 3 (2007) 300-304.
- [6] M.A. Khan, H.T. Jung, O.B. Yang, Synthesis and characterization of ultrahigh crystalline TiO₂ nanotubes, *J. Phys. Chem. B* 110 (2006) 6626-6630.
- [7] Y.S. Chen, J.C. Crittenden, S. Hackney, L.Sutter, D.W. Hand, Preparation of a novel TiO₂-based p-n junction nanotube photocatalyst, *Environ. Sci. Technol.* 39 (2005) 1201-1208.
- [8] T. Kasuga, M. Hiramatsu, A. Hoson, T. Sekino, K. Niihara, Titania nanotubes prepared by chemical processing, *Adv. Mater.* 11 (1999) 1307-1311.
- [9] G.H. Du, Q. Chen, R.C. Che, Z.Y. Yuan, L.M. Peng, Preparation and structure analysis of titanium oxide nanotubes, *Appl. Phys. Lett.* 79 (2001) 3702-3704.
- [10] B.B. Lakshmi, C.J. Patrissi, C.R. Martin, Sol-gel template synthesis of semiconductor oxide micro- and nanostructures, *Chem. Mater.* 9 (1997) 2544-2550.
- [11] V. Zwillig, E. Darque-Ceretti, A. B. Forveille, D. David, M. Y. Perrin¹, M. Aucouturier, Structure and physicochemistry of anodic oxide films on titanium and TA6V alloy, *Surf. Interface Anal.* 27 (1999) 629-637.
- [12] R.A. Caruso, J.H. Schattka, A. Greiner, Titanium dioxide tubes from sol-gel coating of electrospun polymer fibers, *Adv. Mater.* 13 (2001) 1577-1579.
- [13] D.W. Gong, C.A. Grimes, O.K. Varghese, W.C. Hu, R.S. Singh, Z. Chen, E.C. Dickey, Titanium oxide nanotube arrays prepared by anodic oxidation, *J. Mater. Res.* 16 (2001) 3331-3334.

- [14] G.K. Mor, O.K. Varghese, M. Paulose, K. Shankar, C.A. Grimes, A review on highly ordered, vertically oriented TiO₂ nanotube arrays: Fabrication, material properties, and solar energy applications, *Sol. Energ. Mat. Sol. C.* 90 (2006) 2011-2075.
- [15] G.K. Mor, K. Shankar, M. Paulose, O.K. Varghese, C.A. Grimes, Enhanced photocleavage of water using titania nanotube arrays, *Nano Lett.* 5 (2005) 191-195.
- [16] G.K. Mor, O.K. Varghese, M. Paulose, K.G. Ong, C.A. Grimes, Fabrication of hydrogen sensors with transparent titanium oxide nanotube-array thin films as sensing elements, *Thin Solid Films* 496 (2006) 42-48.
- [17] C. Dechakiatkrai, J. Chen, C. Lynam, S. Phanichphant, G.G. Wallace, Photocatalytic oxidation of methanol using titanium dioxide/single-walled carbon nanotube composite, *J. Electrochem. Soc.* 154 (2007) A407-411.
- [18] X. Quan, S.G. Yang, X.L. Ruan, H.M. Zhao, Preparation of titania nanotubes and their environmental applications as electrode, *Environ. Sci. Technol.* 39 (2005) 3770-3775.
- [19] Y.K. Lai, L. Sun, Y.C. Chen, H.F. Zhuang, C.J. Lin, J.W. Chin, Effects of the structure of TiO₂ nanotube array on Ti substrate on its photocatalytic activity, *J. Electrochem. Soc.* 153 (2006) D123-127.
- [20] H.Y. Zhu, X.P. Gao, Y. Lan, D.Y. Song, Y.X. Xi, J.C. Zhao, Hydrogen titanate nanofibers covered with anatase nanocrystals: A delicate structure achieved by the wet chemistry reaction of the titanate nanofibers, *J. Am. Chem. Soc.* 126 (2004) 8380-8381.
- [21] J.G. Yu, H.G. Yu, B.Cheng, C. Trapalis, Effects of calcination temperature on the microstructures and photocatalytic activity of titanate nanotubes, *J. Mol. Catal. A* 249 (2006) 135-142.
- [22] J.G. Yu, X.J. Zhao, Q.N. Zhao, Photocatalytic activity of nanometer TiO₂ thin films prepared by the sol-gel method, *Mater. Chem. Phys.* 69 (2001) 25-29.

- [23] T. Uchikoshi, T.S. Suzuki, F. Tang, H. Okuyama, Y. Sakka, Crystalline-oriented TiO₂ fabricated by the electrophoretic deposition in a strong magnetic field, *Ceramic Inter.* 30 (2004) 1975-1978.
- [24] D. Eder, I.A. Kinloch, A.H. Windle, Pure rutile nanotubes, *Chem. Commun.* 13 (2006) 1448-1450.
- [25] M.M. Wu, J.B. Long, A.H. Huang, Y.J. Luo, Microemulsion-mediated hydrothermal synthesis and characterization of nanosize rutile and anatase particles, *Langmuir* 15 (1999) 8822-8825.
- [26] O.K. Varghese, D. Gong, M. Paulose, C.A. Grimes, E.C. Dickey, Crystallization and high temperature structural stability of titanium oxide nanotube arrays, *J. Mater. Res.* 18 (2003) 156-165.
- [27] F.Z. Hui, J.L. Chang, K.L. Yue, L. Sun, J. Li, Some critical structure factors of titanium oxide nanotube array in its photocatalytic activity, *Environ. Sci. Technol.* 41 (2007) 4735-4740.
- [28] H.T. Chang, N. Wu, F. Zhu, A kinetic model for photocatalytic degradation of organic contaminants in a thin film TiO₂ catalyst, *Water Res.* 34 (2000) 407-416.
- [29] Y.J. Chen, D.D. Dionysiou, Correlation of structural properties and film thickness to photocatalytic activity of thick TiO₂ films coated on stainless steel, *Appl. Catal. B* 69 (2006) 24-33.
- [30] W. Chen, Z.G. Wang, Z.J. Lin, L.Y. Lin, Absorption and luminescence of the surface states in ZnS nanoparticles, *J. Appl. Phys.* 82 (1997) 3111-3115.
- [31] R.N. Bhargava, D. Gallaghr, X. Hong, A. Nurmikko, Optical properties of manganese-doped nanocrystals of ZnS, *Phys. Rev. Lett.* 72 (1994) 416-419.
- [32] R.F. Chen, L. Zhang, Y. Wei, D.L. Hou, Preparation of rutile (TiO₂) nanostructured materials at low temperature from TiCl₄ aqueous solution, *J. Mater. Sci.* 42 (2007) 714-7146.

[33] M. Qamar, C.R. Yoon, H.J. Oh, N.H. Lee, K. Park, D.H. Kim, K.S. Lee, W.J. Lee, S.J. Kim,
Preparation and photocatalytic activity of nanotubes obtained from titanium dioxide, *Catal.*
Today 131 (2008) 3-14.

List of figure captions

Figure 1. FESEM images of samples calcined at 500 °C for 1 h. (The anodization conditions for different samples are listed in Table 1.)

Figure 2. XRD patterns of fresh Ti foil and TNT-S5 samples calcined at different temperatures:
A- anatase; R- rutile; T- titanium.

Figure 3. FESEM images of TNT-S5 sample calcined at 800 °C.

Figure 4. XPS spectrum of TNT-S5 sample calcined at 500 °C for 1 h in air.

Figure 5. Effect of surface structures of anodized TNT films on the photocatalytic degradation of 2,3-DCP under UV light irradiation ($C_0 = 20 \text{ mg L}^{-1}$).

Figure 6. Effect of TiO₂ nanotube length on the photocatalytic degradation of 2,3-DCP under UV light irradiation ($C_0 = 20 \text{ mg L}^{-1}$).

Figure 7. Effect of TiO₂ nanotube wall thickness on the photocatalytic degradation of 2,3-DCP under UV light irradiation ($C_0 = 20 \text{ mg L}^{-1}$).

Figure 8. Dependence of rate constant (k) of TNT-S5 on the calcination temperature. (All correlation coefficient (R^2) values are higher than 0.98.)

Table 1

Anodization conditions and the size of TiO₂ nanotubes

Sample ID	V ^a (v)	t ^b (h)	T ^c (°C)	WT ^d (nm)	L ^e (μm)
TNT-S1(500) ^f	10	1	23	–	–
TNT-S2(500)	15	1	23	40 ± 5	0.29 ± 0.05
TNT-S3(500)	18	1	23	30 ± 5	0.32 ± 0.05
TNT-S4(500)	25	0.3	23	35 ± 5	0.20 ± 0.03
TNT-S5(500)	25	1	23	28 ± 5	0.31 ± 0.03
TNT-S6(500)	25	10	23	33 ± 5	2.38 ± 0.05
TNT-S7(500)	25	1	5	50 ± 5	0.32 ± 0.04

^a Applied voltage; ^b Reaction time; ^c Reaction temperature; ^d Wall thickness of nanotubes;^e Length of nanotubes; ^f Samples calcined at 500 °C for 1 h.

Fig. 1

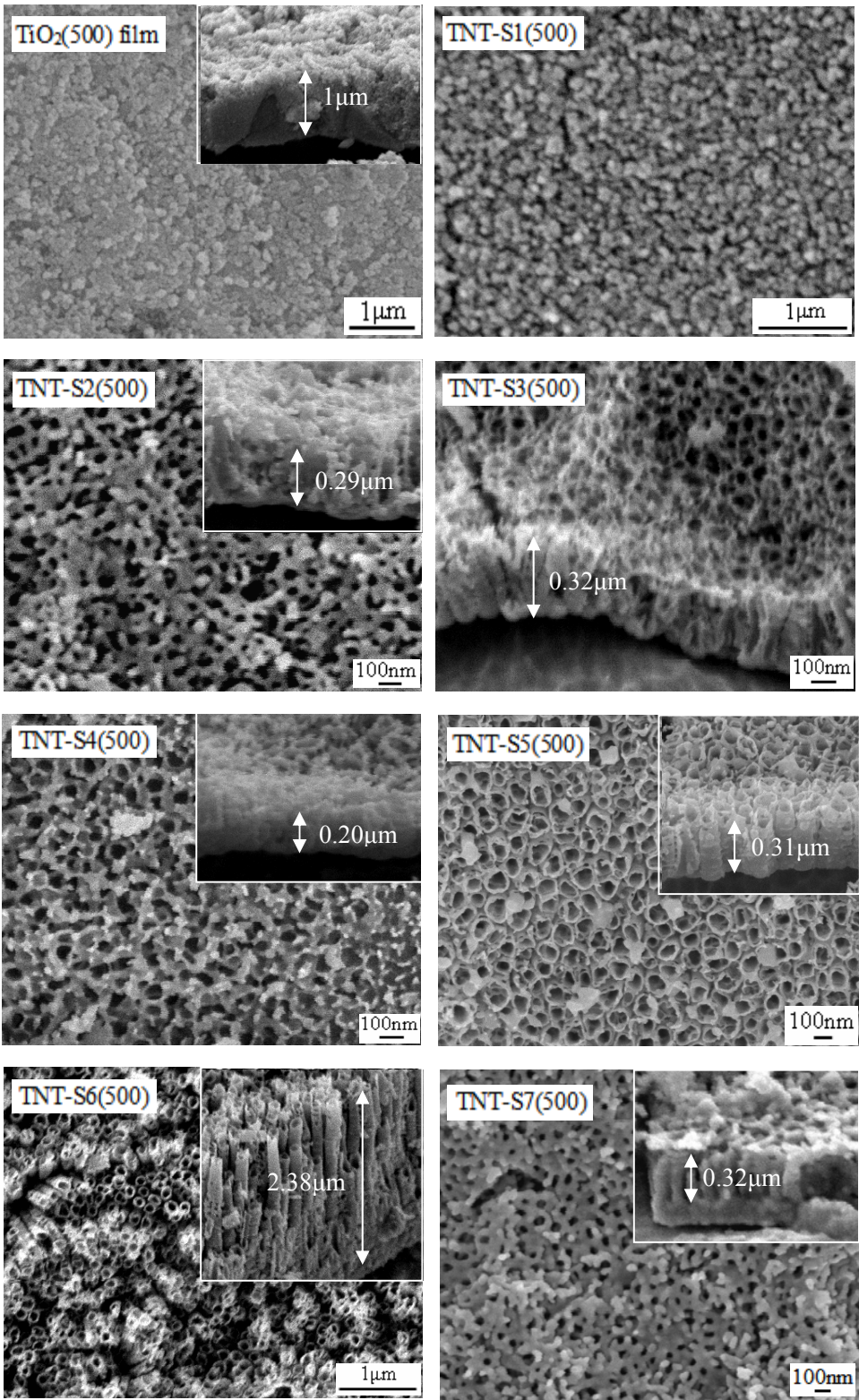


Fig. 2

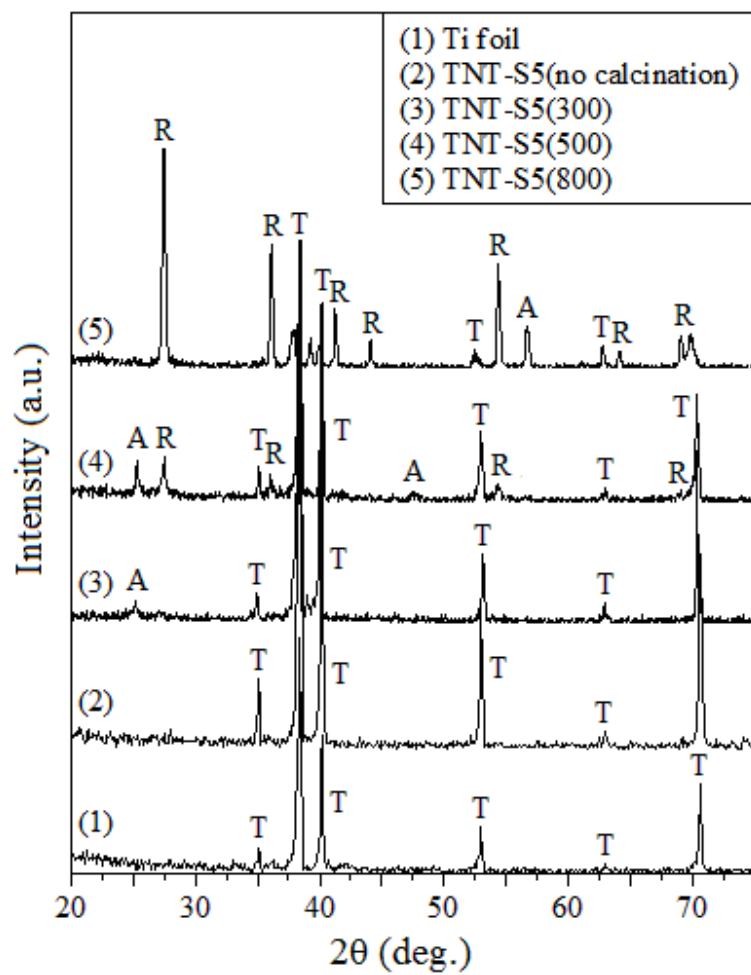


Fig. 3

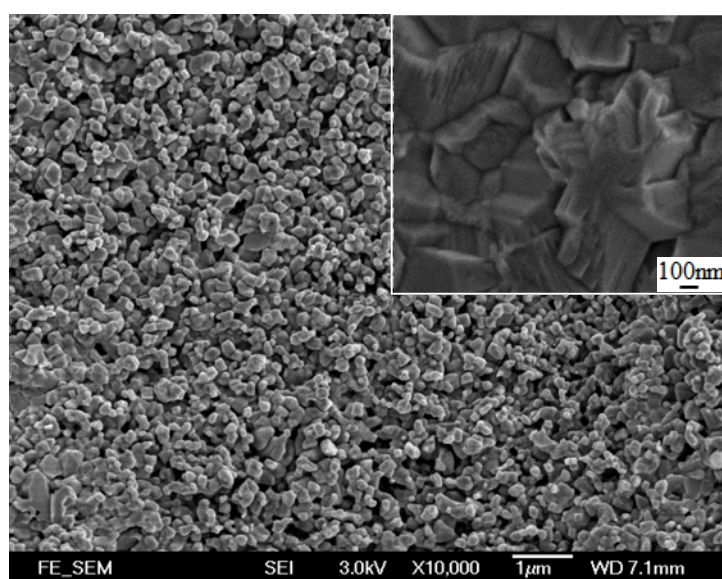
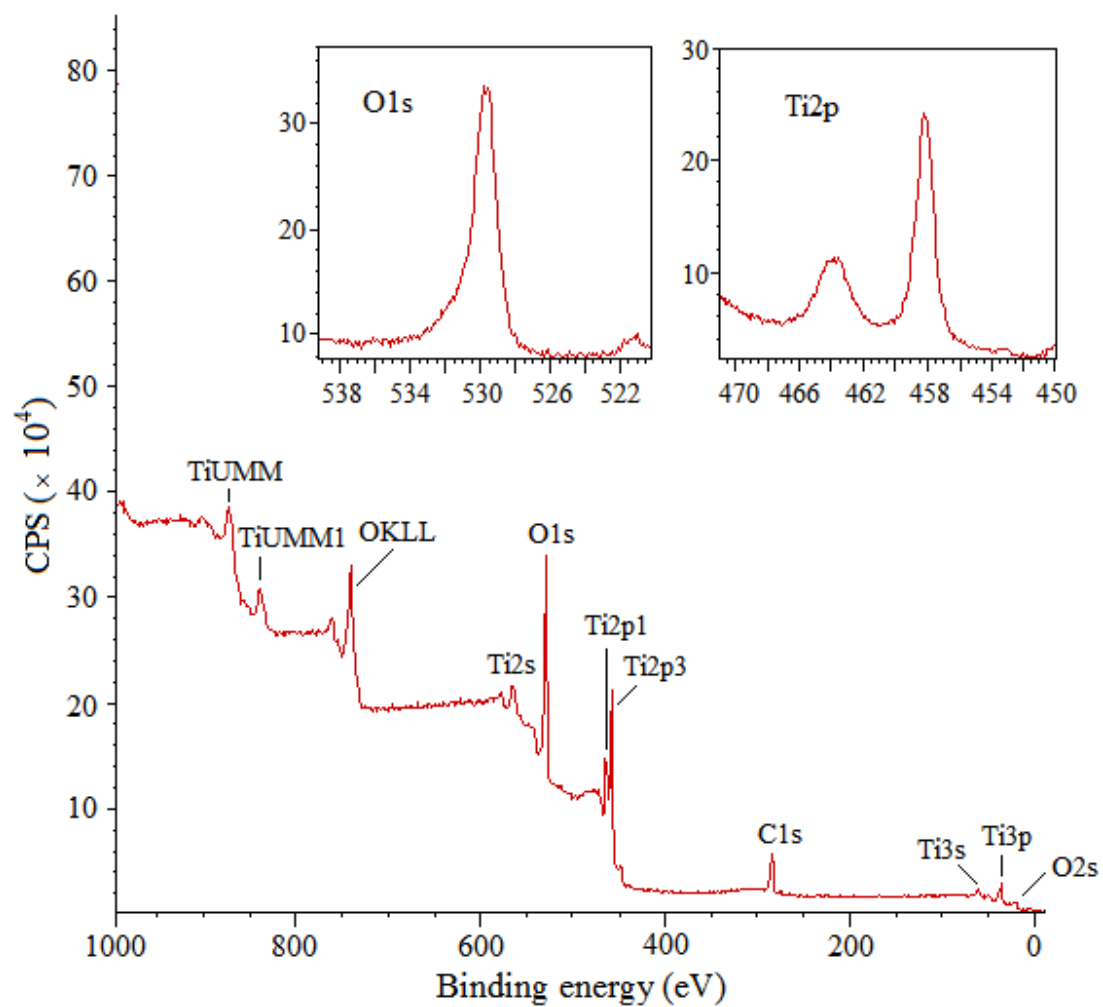


Fig. 4



(The color figure is intended to be reproduced in black-and-white.)

Fig. 5

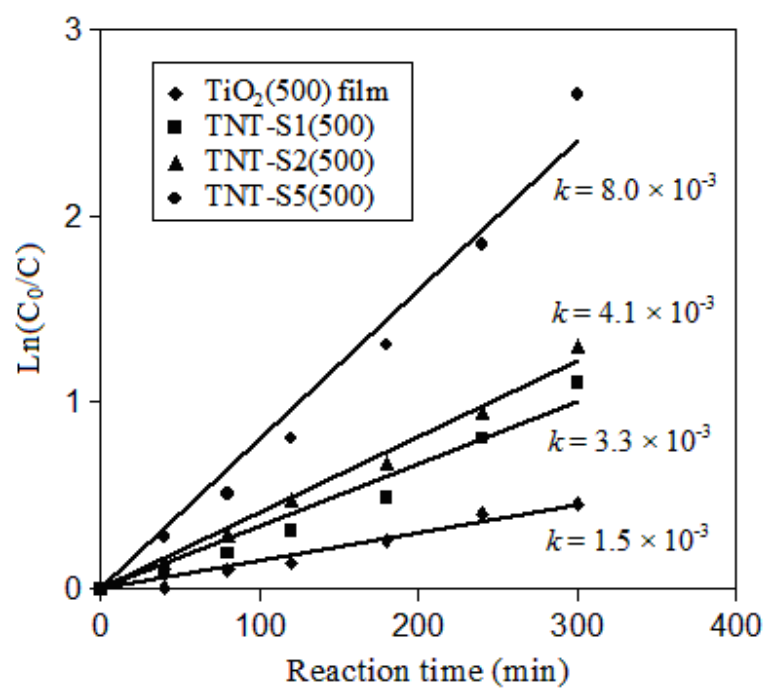


Fig. 6

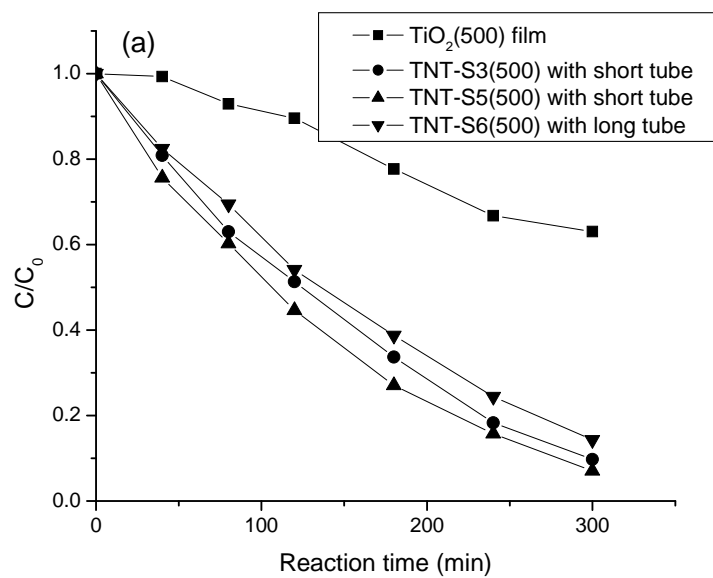


Fig. 7

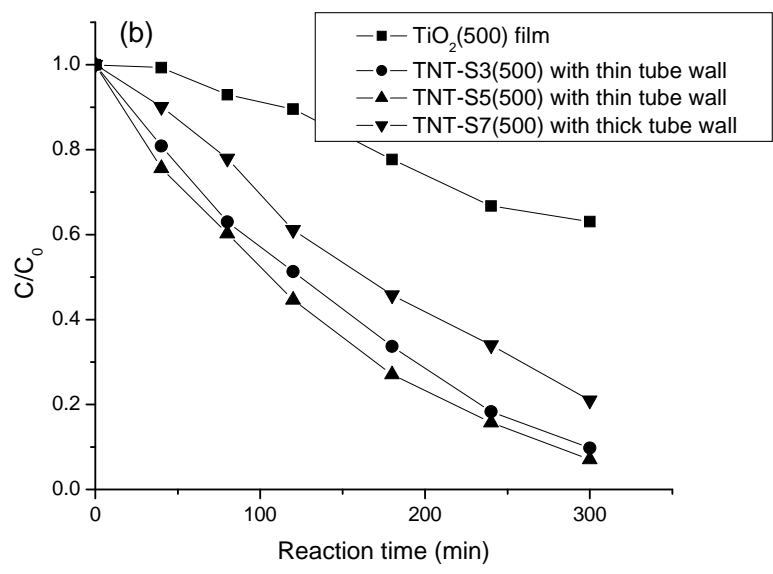


Fig. 8

